LAWRENCE
LIVERMORE
NATIONAL
LABORATORY

LLNL-JRNL-426863

Photoacoustically Measured Speeds of Sound of Liquid HBO2: On Unlocking the Fuel Potential of Boron

Sorin Bastea, Jonathan Crowhurst, Michael Armstrong, Nick Teslich Jr.

April 1, 2010

Science or Journal of Physical Chemistry Letters (not sure yet)

Disclaimer

Photoacoustically Measured Speeds of Sound of Liquid HBO_2: On Unlocking the Fuel Potential of Boron

Joseph M. Zaug, Sorin Bastea, Jonathan C. Crowhurst, Michael R. Armstrong, and Nick E. Teslich Jr.*

Lawrence Livermore National Laboratory, Physical and Life Sciences, PO BOX 808, L-350, Livermore CA 94551

AUTHOR EMAIL ADDRESS zaug1@llnl.gov

RECEIVED DATE (to be automatically inserted after your manuscript is accepted if required according to the journal that you are submitting your paper to)

* To whom correspondence should be addressed. E-mail: zaug1@llnl.gov

ABSTRACT Elucidation of geodynamic, geochemical, and shock induced processes is often limited by challenges to accurately determine molecular fluid equations of state (EOS). High pressure liquid state reactions of carbon species underlie physiochemical mechanisms such as differentiation of planetary interiors, deep carbon sequestration, propellant deflagration, and shock chemistry. Here we introduce a versatile photoacoustic technique developed to measure accurate and precise speeds of sound (SoS) of high pressure molecular fluids and fluid mixtures. SoS of an intermediate boron oxide, HBO_2 are measured up to 0.5 GPa along the 277 ˚C isotherm. A polarized Exponential-6 interatomic potential form, parameterized using our SoS data, enables EOS determinations and corresponding semi-empirical evaluations of > 2000 ˚C thermodynamic states including energy release from bororganic formulations. Our thermochemical model propitiously predicts boronated hydrocarbon shock Hugoniot results.

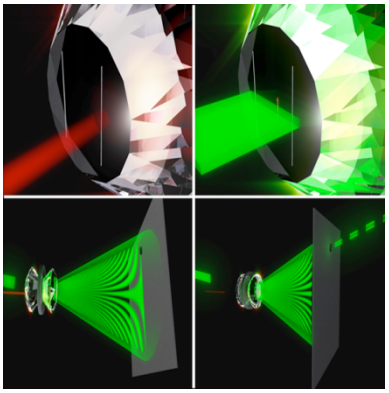

KEYWORDS HBO_2, Speed of Sound, High Pressure Equation of State, Photoacoustic Light Scattering, Chapman-Jouguet, Thermochemical, Exponential-6, Double-slit experiment

Fluid state high-pressure and temperature physiochemical processes involving metallic and carbon containing reactants are ubiquitous in nature and command the interests of an extraordinary range of interdisciplinary and technological endeavors e.g., astro- planetary- geo- and atmospheric sciences, nuclear engineering, combustion and high explosive materials science, and explosive crystallization of technologically important materials to name but just a few.[1–7] Quantitative predictions of extreme-condition chemistry are inexorably linked to knowing EOS of probable major reaction species. For example, the optimal use of metal fuel additives to enhance the release of chemical energy stored in organic crystals has been stymied by the lack of oxide component EOS data. Aluminum (Al) powder has long been proposed as a promising candidate fuel to significantly increase chemical power output of highly energetic (HE) material formulations.[8] Large-scale tests revealed that Al additives actually decrease shock pressure and reaction velocities of HEs, an effect later attributed to low heat of formation oxide products at the Chapman-Jouguet (C-J) state of explosives, i.e. the thermodynamic state where reaction products behind a steady propagating detonation front reach chemical equilibrium.[6] It is now well understood that exothermic reactions must meet or exceed high melt temperatures of metal oxides before fuel enhancement can be achieved. Inability to realize the full potential of Al fuel lead to consideration of utilizing boron, which has the highest elemental heat of combustion ΔH = 137.45 kJ/cc,per unit volume.[9] Combustion enhancement using boron has also proved difficult to harness; the complete oxidation of boron can be poisoned by the presence of a common reaction product, water vapor.[10] To sufficiently elucidate the chemical energy landscape of metalized propellants or HEs the efficacy of controlled parameters, e.g., metal powder grain size and concentration, pure metal powder vs. metal fractionated compounds, oxidizer and fluorinator concentration, etc. continue to be examined using combustion or large-scale tests. Macroscopic-scale performance metrics e.g., energy release and reaction rate, of tested formulations provides necessary information required to challenge predictions made using EOS based thermochemical models. Thus stringently refined semi-empirical computational models serve to guide and reduce time consuming and dangerous investigations of new formulations.

The study of combustion reactions involving boron has lead to the conclusion that a simple molecular product HBO_2, affects to a significant degree the energy output since it is an effective molecular trap to boron on its path to full oxidation.[11] We hypothesize that HBO_2 will likely have a similar effect on the properties of boron containing HEs. Despite decades of study however there are no EOS type data available of HBO_2 to test such predictions. We present in this paper the first such experimental results on the SoS of HBO_2 at elevated pressures and temperatures. Normally we apply the impulsive stimulated light scattering (ISLS) technique to generate and probe acoustic wave propagation in fluid samples encapsulated within resistively heated diamond-anvil cells (DAC).[12-14] However there are practical limitations to the ISLS technique applied to optically thin, e.g., <50 μm fluids, 1) they must absorb minimally some of excitation-pulse light and, 2) exhibit no photo reactions with either excitation- or probe-pulses. Unfortunately HBO_2(l) does not absorb the fundamental or higher harmonics of our 1064 nm excitation source. Furthermore we observe a high propensity for HBO_2 photochemistry induced by exposure to overlapped ISLS excitation pulses (1.0-1.4 GW/cm^2 peak Gaussian profile irradiance) –these issues are common to most fluids over a wide range of available visible to near-IR laser wavelengths.

In this report we introduce a time-domain (T-D) photoacoustic light scattering (PALS) technique to enable in situ SoS measurements from optically thin materials encapsulated under non ambient pressure-temperature conditions. The accuracy of PALS is first established by comparison of H_2O(l) and H_2O(s) SoS measurements with literature results and, in turn, HBO_2(l) results are given to establish an EOS. Advantages of PALS over Brillouin or ISLS approaches are (i) low average irradiance, (1-3 orders of magnitude less than CW laser Brillouin measurements) and low peak irradiance (1-2 orders of magnitude less than pulsed laser transient grating measurements), which significantly reduces the potential for photochemical initiated reactions (ii) inherently low frequency measurements, which helps to avoid or minimize liquid-state acoustic dispersion affects, (iii) at least one order of magnitude in tunable frequency range is available to conduct acoustic dispersion studies that can be very rapidly conducted on glasses and polymers to reveal structural relaxation rates without need to alter incoming

beam angles, wavelengths or the sample position, (iv) optically thin e.g., 5 μm materials can easily be studied with no requirement to absorb excitation- or probe-pulse wavelengths. The technical advantages of using T-D SoS techniques for the study of fluids have been previously discussed.[12] Here we provide SoS data from a material that is highly susceptible to laser-induced photochemistry using an experimental approach that is highly versatile and straightforward to execute.

A PALS transducer is made by depositing a platinum film onto the culet of a diamond-anvil. Focused ion beam (FIB) site-specific deposition is conducted using a FEI Nova600i NanoLab instrument. A culet is first cleaned and then coated with 150-200 Å of carbon to minimize FIB charging effects. A precursor gas, trimethyl platinum (TMP) is introduced approximately 200 μm above a culet surface. TMP interacts with a scanning ion beam whereby Pt deposition ensues at the culet surface. We initially found that four parallel Pt transducers, (0.5-1.0 μm wide, approximately 75 μm long, and 0.27-μm tall), with center-to-center line separations of 22, 25, 30, and 33 μm enable one to measure speeds of sound with velocities ranging from 0.5 to at least 5 km/sec (Figure 1a, 1b). Welding micron dimensional wire onto one anvil by method of compression with an opposing anvil may also work to form a transducer.

To generate sound, a 100 ps optical pulse is focused onto a transducer. The peak laser irradiance, <0.03 GW/cm^2, impulsively increases temperature in the transducer (electron-phonon energy transfer) by a few degrees. The temperature rise produces a thermal stress distribution in the Pt film that launches a longitudinal strain-pulse. The pulse energy is reflected and transmitted at the interface between the film and the surrounding sample. Transmitted broadband pulses that travel perpendicular to the direction of the excitation-pulse and into the surrounding medium are utilized to make SoS measurements. The physics behind similar photoacoustic transducers is well documented however the geometry and application of our device is unique.[15-18] At 277 °C and 0.01GPa, the acoustic impedance of Pt ≈ 8.8.0x10^7 Kg/s·m^2 and HBO_2(l) = 6.5x10^5 Kg/s·m^2 and so the transmitted acoustic intensity I_T of that initially within the film is 2.9%; generally I_T increases with applied pressure because fluids are more compressible than metal, e.g., $I_T \approx 4.2\%$ at 0.5 GPa. The traveling acoustic peak (expansion of the

medium) increases and the acoustic trench (rarefaction following expansion of the medium) reduces the nominal index of refraction of the sample and therefore alters the local magnitude of optical diffraction. A time-of-flight delayed 532 nm probe-pulse (~ 20 μm FWHM spot) is focused onto a second and parallel Pt film. Each T-D datum represents the average of at least 800 laser shots and each time series is 500-800 points in length. (In principle, a CW laser probe and a sufficiently fast GHz range detector and oscilloscope could be employed to collect an entire T-D series in real-time.) Probe radiation scatters off of the Pt films forming a local oscillator (LO) or reference field, E_R, (I_R=E_R^2) with a constant phase. Probe radiation also diffracts from the traveling wave, generating a diffracted field, E_D (I_D=E_D^2) with a time-varying phase. A pin-hole aperture is positioned behind the DAC to select a signal collection wave-vector, K_S and pass a narrow cone of light (<1x10^{-4} % of the available DAC solid angle) to a photomultiplier tube, (PMT). Signal intensity measured at the PMT is equal to the square of the mixed (heterodyne detection) fields, and is modulated by the time varying optical phase difference between E_R and E_D.[19] Here the frequency of the material response is given by $\nu_A = 2c/\lambda_P$ ($\sin\theta/2$), where c is the adiabatic SoS, λ_P is the probe wavelength, and $\theta = \theta_{Pi} + \theta_{Pd}$, the probe angle of incidence and the probe angle of diffraction. The phenomenon described here is analogous to Thomas Young's well-known double-slit diffraction experiment where here the slit separation, i.e. the distance between the traveling wave and the point where I_R is generated, is time dependant.[20] Time-domain series (Fig. 2a) are Fourier transformed to compute modulation frequency (ν_A < 2 GHz for θ = 10°, c ≤ 6 km/sec, λ_P = 532 nm). A Web-enhanced object, an animation, of the PALS process is available in Quicktime format.

The selected value of K_S is determined by conducting PALS measurements from water where accurately established $c(P,T)$ data are published. PALS measurements compare favorably to the well-established IAPWS-95 formulations (standard deviation is 0.6%) including accurate ISLS results (Figure 2b).[14,21,22] A powerful feature of PALS allows for a continuum of K_S values to be accessed for rapid investigations of dispersion relations without need to physically change θ_{Pi} or the sample position (ν_A = 0.4 – 4.0 GHz for θ = 5° - 53°, c = 2.4 km/sec, and λ_P = 0.532 μm). High P-T SoS are determined

by, $c = \nu_A / K_S$. Recent improvements, e.g., the use of a cylindrical probe profile, have reduced the error to <0.5%.

The molecular stability of HBO_2 was verified by μ-FTIR up to 277 ˚C and 0.7 GPa. At 277 ˚C HBO_2 begins to slowly freeze above 0.22 GPa. In this pressure range the interpolated melting curve is relatively steep, 490 ˚C/GPa. Above 300-350 ˚C, fluorescent optical manometers consistently failed within 60 minutes; perhaps the oxidation potential of the fluid increased. The narrow P-T region where precise fluid-state HBO_2 measurements are accessible may explain the lack of any previous data. SoS results for HBO_2(l) are plotted in Fig. 3.

The SoS data provide an opportunity for deriving effective intermolecular interactions for the HBO_2 product, thus enabling accurate predictions of thermodynamic and chemical equilibrium states of highly energetic reactions involving boron containing or loaded compounds. To this end we employ an EXP6-polar thermodynamics theory that was previously shown to yield very good results for the properties of hot, dense water as well as those of HNO_2.[23,24] HBO_2 is also a strongly polar molecule, with a dipole moment larger than H_2O; for the purpose of modeling HBO_2 we set the value of its dipole moment to the calculated value for the isolated molecule, $\mu = 2.78$ Debye.[25] It is possible and quite likely that, similarly with H_2O, a somewhat larger value of μ may be more appropriate for describing HBO_2 at the high density fluid conditions typical of detonation or high pressure combustion, whose properties we eventually wish to predict. However, the limited experimental data presently available do not warrant trying to discern such an effect; we expect that this approximation will have little effect on our conclusions regarding the character of detonations containing boron, which at this point can only be largely qualitative. We find that EXP6 parameter values, $r_o = 3.976$ Å, $\varepsilon = 216.3$ K, and $\alpha = 12.67$ using the above dipole moment yield good agreement with the SoS measurements - see Figure 3. Thermodynamic calculations using these parameters place the critical point of HBO_2 approximately at T_c = 447 ˚C and P_c = 260 atm; of course chemical reactivity may actually intervene before these conditions can be reached.

The important role that molecular HBO_2 is likely to play in hydrocarbon or organometallic explosive combustion of boron particles (e.g. in rocket propellants and ramjet fuels) is well documented.[9, 11, 26-30] Here we attempt to quantify its impact in the detonation of explosives containing elemental boron by employing the newly determined HBO_2 thermodynamics in the calculation of detonation velocities. These calculations are performed using the code CHEETAH and are similar with those described for example in Ref. 31. The code is used here to determine C-J points of explosives. Detonation product results are constrained to single-phase fluid mixtures and, potentially, many condensed phases. The major boron-containing products likely to be relevant for such processes have been discussed for example by Akimov et al..[32] The fluid phase components we consider are small molecular products such as N_2, CO_2, H_2O, CO, NH_3, CH_4, HBO_2, O_2, H_2, etc., which are thermodynamically favored at high temperatures and pressures; they are all modeled by EXP6 or EXP6-polar interactions and tested favorably against experimental data. The condensed phases are carbon (diamond and graphite), B_2O_3 (liquid and solid), B (solid and liquid), BN (cubic and hexagonal solids), CB_4 (solid) and H_3BO_3 (solid), all described by Murnaghan-type EOS. Among these B_2O_3 is of particular importance; it is likely the oxidation end-point of boron. Unfortunately B_2O_3 experimental data are very scarce. We note however that our liquid EOS is in good agreement with the simulation results of Ohmura et al., and the melting line agrees well with that reported by Brazhkin et al. (Figure. 4a).[33,34] Nevertheless, such uncertainties due to the lack of EOS data for likely major reaction products, probably limit our ability to make fully quantitative predictions.

The combustion of solid boron particles is plagued by well known kinetics issues, which are likely to also be important in the detonation of explosives loaded with metallic boron, just as in the case of aluminum-loaded compositions.[35] We attempt to circumvent these complications and focus therefore on explosive mixtures with boronated organic compounds, which were studied experimentally.[32] These are, 1) 86% (by weight) pentaerythritol tetranitrate ($C_5H_8N_4O_{12}$) + 14% orthocarborane ($C_2B_{10}H_{12}$), 2) 75% tetranitromethane (CN_4O_8) + 25% pentaborane (B_5H_9), and 3) 70% tetranitromethane + 30% borazine ($B_3N_3H_6$); their initial densities are ρ_o = 0.78, 1.14, and 1.28 g/cc, respectively. The experimental

detonation velocities reported are D_{exp}=4.64, 5.9, and 6.3 km/s; our corresponding calculated values are D_{calc} = 4.78 (Δ=3.02%), 5.96 (Δ=1.02%) and 6.13 (Δ=-2.70%) km/s, respectively, indicating reasonable agreement. For these energetic mixtures we find that the major detonation products containing boron are HBO_2 and B_2O_3(l) (mixture two also yields a small amount of liquid boron), mixed with the molecular detonation products typical for CHNO explosives. We show for example in Figure 4b the C-J region composition of mixture 3), which indicates, as expected, that large amounts of water also result upon detonation. Since the reaction of B_2O_3 (l) with water is likely an important route toward the formation of HBO_2, its study at high temperatures and pressures will significantly increase the confidence of quantitative predictions of the thermodynamic and kinetic behavior of boron containing explosives and propellants.[10]

Our study reveals that the reaction of B_2O_3 (l) + H_2O(v) is a plausible route toward the formation of HBO_2 under detonation conditions. Previously the collection of accurate SoS data using in situ measurement techniques was hindered by materials that exhibit high photosensitivity and/or limited P-T regions of chemical stability. SoS data from HBO_2(l), suggest, that we can utilize EOS based thermochemical models to predict high-pressure combustion, deflagration, and detonation chemistry involving boron: a reasonable level of confidence for computing metal assisted high-energy reactions has been achieved. We also make note that in situations where a carbon deficient oxidizer e.g., ammonium perchlorate (NH_4ClO_4), reacts with 10 % wt. boron, our calculations predict up to five times more HBO_2 product is likely to be found compared to results given above –an expected result given that the concentration of oxygen competing carbon products, e.g. CO, CO_2, is severely diminished. We expect that the relative simplicity and high versatility of PALS type measurements will assist research initiatives directed to understand a wide-array of extreme condition chemical processes.

ACKNOWLEDGMENT J. M. Z. is grateful to L. E. Fried, J. M. Brown, and E. H. Abramson for stimulating and thoughtful discussions. This research was funded by the DOE Campaign-II and Joint DoD/DOE Munitions Technology Programs and performed under the auspices of the U.S. Department of Energy by Lawrence Livermore National Laboratory under contract DE-AC52-07NA27344. The authors thank Kimberly Budil, now senior advisor to the Under Secretary for Science at the U. S. DOE, and Bruce Watkins, LLNL program manager, for their continued support of our research.

(a) (b)

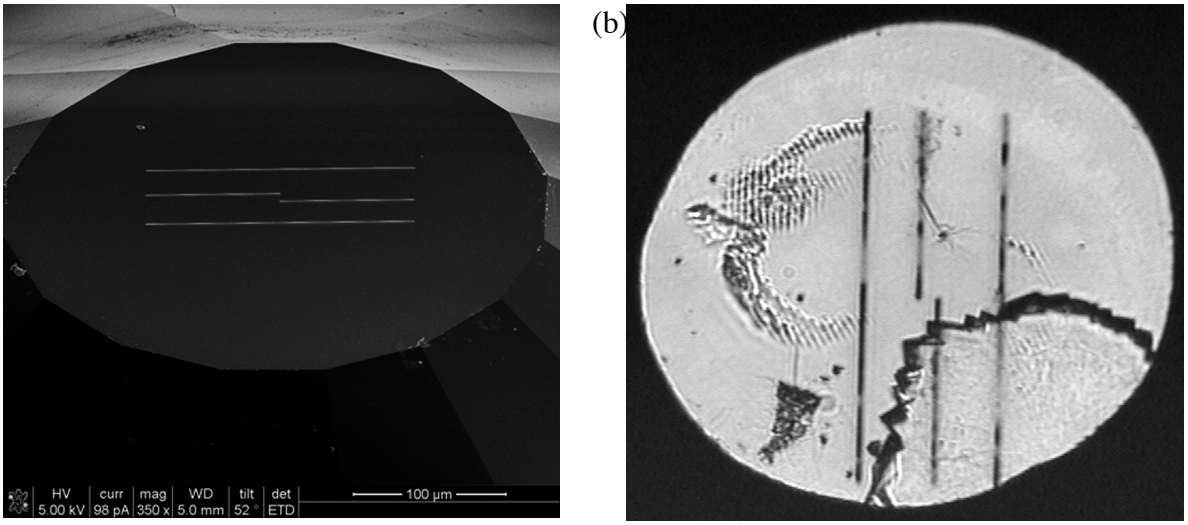

Figure 1. (a) A TEM image of platinum films deposited onto a diamond-anvil. (b) A photo-micrograph of a DAC sample chamber. At 0.4 GPa and 277 ˚C solid HBO_2 slowly encroaches on the supercooled fluid. Inspection of the left side of the chamber reveals gratings that were burned into the culet from failed attempts to generate traditional ISLS signals. A pressure manometer rests in the lower left region of the chamber.

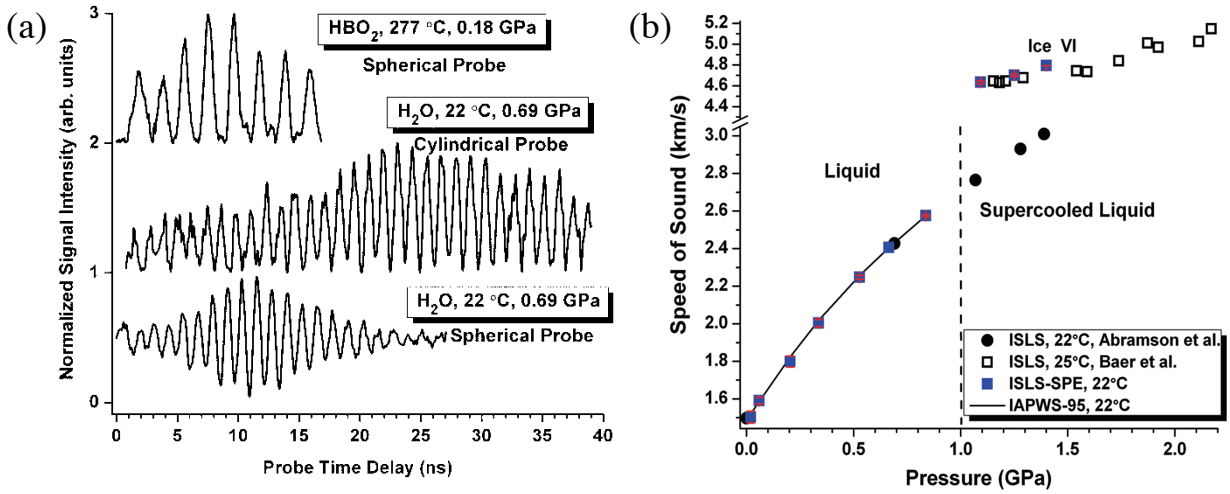

Figure 2. (a) PALS time-domain signals from liquid H_2O and HBO_2. (b) Determination of K_S is accomplished by measuring ν_A from a sample of known c(P,T). K_S was selected using the IAPWS-95 value for H_2O SoS at 0.66 GPa and 22 °C; PALS results compare well with liquid and solid state measurements of Abramson and Baer.[14, 21, 22]

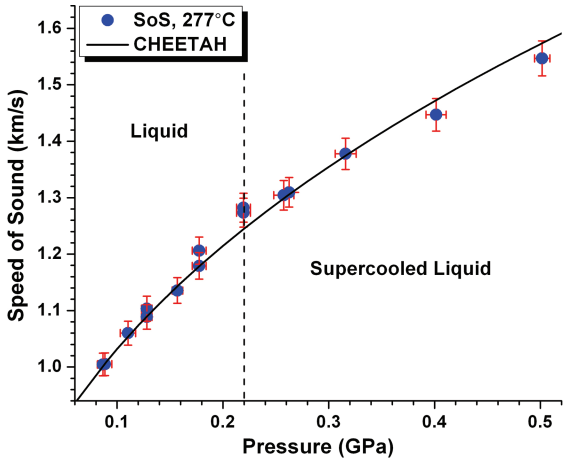

Figure 3. Measured SoS from HBO_2(l), filled circles, and calculated SoS from EXP6-polar function, solid line.

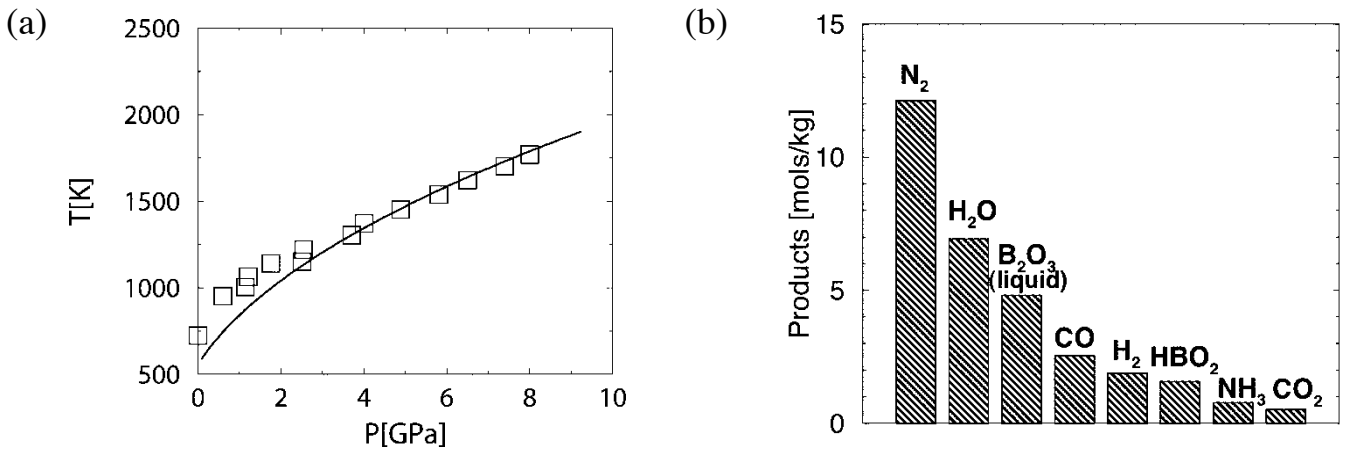

Figure 4. (a) Calculated B_2O_3 melt curve from CHEETAH (solid line) compared to experimental data (open squares) from Brazhkin et al..[34] (b) Calculated C-J plane decomposition mixture from 70% tetranitromethane + 30% borazine ($B_3N_3H_6$).

REFERENCES

(1) Drake M. J.; Richter K. Determining the Structure of the Earth. *Nature* **2002**, 416, 39-44.

(2) Bergeron P.; Saumon D.; Wesemael F. New Model Atmospheres for Very Cool White Dwarfs with Mixed H/He and Pure He Compositions. *Astrophysical Journal* **1995**, 443, 764-779.

(3) Cavazzoni C.; Chiarotti G. L.; Scandolo S.; Tosatti E.; Bernasoni M.; Parrinello M. Superionic and Metallic States of Water and Ammonia at Giant Planet Conditions. *Science* **1999**, 283, 44-46.

(4) Koshizuka S.; Ikeda H.; Oka Y. Numerical Analysis of Fragmentation Mechanisms in Vapor Explosions. *Nuclear Engineering and Design* **1999**, 189, 423-433.

(5) Clupara D.; Lyubovsky M. R.; Altman E.; Pfefferie L. D.; Datye A. Catalytic Combustion of Methane over Palladium-Based Catalysts. *Cat. Rev.-Sci. and Eng.* **2002**, 44, 593-649.

(6) Fickett W.; Davis W. C. Detonation Theory and Experiment. Dover Publications: Mineola New York, 1979.

(7) Albenze E. J.; Thompson M. O.; Clancy P. Molecular Dynamics Study of Explosive Crystallization of SiGe and Boron-Doped SiGe Alloys. *Ind. Eng. Chem. Res.* **2006**, 45, 5628-5639.

(8) Cook M. A.; Filler A. S.; Keyes R. T.; Partridge W. S.; Ursenbach W. O. Aluminized Explosives. *J. Chem. Phys.* **1957**, 61, 189-196.

(9) Peretz A Some Theoretical Considerations of Metal-Fluorocarbon Compositions for Ramjet Fuels. Proceedings of the Eighth International Symposium on Air Breathing Engines, Cincinnati, OH, June 14-19, **1987**, 398-403.

(10) Foelsche R. O.; Burton R. L.; Krier H. Boron particle ignition and combustion at 30-150 ATM, *Combustion & Flame* **1999**, 117, 32-58.

(11) Meschi D. J.; Chupka W. A.; Berkowitz J. Heterogeneous reactions studied by mass spectrometry. I. Reaction of B_2O_3(s) with H_2O(g). *J. Chem. Phys.* **1960**, 33, 530-532.

(12) Yan Y.-X.; Nelson K. A. Impulsive stimulated light scattering. II. Comparison to frequency-domain light-scattering spectroscopy. *J. Chem. Phys* **1987**, 87, 6257-6265.

(13) Zaug J. M.; Slutsky L. J.; Brown, J. M. Equilibrium properties and structural relaxation in methanol to 30.4 GPa. *J. Phys. Chem. B* **1994**, 98, 6008-6016.

(14) Abramson E. H.; Brown, J. M. Equation of state of water based on speeds of sound measured in the diamond-anvil cell. *Geochimica Et Cosmochimica Acta* **2004**, 68, 1827-1835.

(15) Tas G.; Maris H. J. Electron diffusion in metals studied by picosecond ultrasonics. *Phys. Rev. B* **1994**, 49, 15046-15054.

(16) Pezeril T.; Ruello P.; Gougeon S.; Chigarev N.; Mounier J. M.; Picart P.; Gusev V. Generation and detection of plane coherent shear picosecond acoustic pulses by lasers: Experiment and theory *Phys. Rev. B*. **2007**, 75, 174307.

(17) Kou C.-Y.; Vieira M. M. F.; Patel C. K. N. Transient optoacoustic pulse generation and detection *J. Appl. Phys*. **1984**, 55, 3333-3336.

(18) Physical Acoustics ed. Mason W. P.; Thurston R. N. Vol. XVIII, Academic Press, INC., 1988.

(19) Crimmons T. F.; Stoyanov N. S.; Nelson K. A. Heterodyned impulsive stimulated Raman scattering of phonon-polaritons in $LiTaO_3$ and $LiNbO_3$ *J. Chem. Phys*. **2002**, 117, 2882-2896.

(20) Young T. The Bakerian lecture: Experiments and calculations relative to physical optics **1804**, *Proc. Royal Soc. London A*, 94, 1-16.

(21) Release of the IAPWS Formulations 1995 for the Thermodynamic Properties of Ordinary Water Substances for General and Scientific Use. *International Association for the Properties of Water and Steam*, **1996**.

(22) Baer B. J.; Brown J. M.; Zaug J. M.; Schiferl D.; Chronister E. L. Impulsive stimulated scattering in ice VI and ice VII. *J. Chem. Phys*. **1997**, 108, 4540-4544.

(23) Bastea S.; Fried L. E. Exp6-polar thermodynamics of dense supercricital water. *J. Chem. Phys*. **2008**, 128, 17502.

(24) Maiti A.; Bastea S.; Howard W. M.; Fried L. E. Nitrous acid under high temperature and pressure – From atomistic simulations to equations of state for thermochemical modeling. *Chem. Phys. Lett*. **2009**, 468, 197-200.

(25) Dewar M. J. S.; JIE C. X.; Zoebisch E. G. AM1 calculations for compounds containing boron. *Organometallics* **1998**, 7, 513-521.

(26) Macek A.; Semple J. M. Combustion of boron particles at atmospheric conditions. *Combustion Science and Technology* **1969**, 1,181-191.

(27) Yetter R. A.; Rabitz F. L.; Dryer F. L.; Brown R. C.; Kolb C. E. Kinetics of high-temperature B/O/H/C chemistry. *Combustion and Flame* **1991**, 83, 43-62.

(28) Ulas A.; Kuo K.; Gotzmer G. Ignition and combustion of boron particles in fluorine-containing environments. *Combustion and Flame* **2001**, 127, 1935-1957.

(29) Spalding M. J.; Krier H.; Burton R. L. Boron suboxides measured during ignition and combustion of boron in shocked Ar/F/O_2 and Ar/N2/O_2 mixtures. *Combustion and Flame* **2000**,120, 200-210.

(30) Sullivan K.; Young G.; Zachariah M. R. Enhanced reactivity of nano-B/Al/CuO MIC's. *Combustion and Flame* **2009**, 156, 302-309.

(31) Scott H. P.; Hemley R. J.; Mao H. K.; Herschbach D. R.; Fried L. E.; Howard W. M.; Bastea S. Generation of methane in the Earth's mantle: In situ high pressure-temperature measurements of carbonate reduction. *Proc. Nat. Acad. Sci. USA* **2004**, 101, 14023-14026.

(32) Akimov L. N.; Apin A. Ya.; Stesik L. N. Detonation of explosives containing boron and its organic derivatives. *Combustion Explosion and Shock Waves* **1972**, 8, 387-390.

(33) Ohmura S.; Shimojo F. Anomalous pressure dependence of self-diffusion in liquid B_2O_3: An ab initio molecular dynamics study. *Phys. Rev. B* **2009**, 80, 020202(R).

(34) Brazhkin V. V.; Katayama Y.; Inamura Y.; Kondrin M. V.; Lyapin A. G.; Popova S. V; Voloshin R. N. Structural transformations in liquid, crystalline, and glassy B_2O_3 under high pressure [JETP Lett. 78 (6), 393-397 (2003)]. *J E T P Lett*. **2004**, 79, 308.

(35) Young G.; Sullivan K.; Zachariah M. R.; Yu K. Combustion characteristics of boron nanoparticles. *Combustion and Flame* **2009**, 156, 322-333.

SYNOPSIS TOC We introduce a highly versatile and straightforward photoacoustic light scattering technique, (PALS) which enables direct time-domain speeds of sound measurements of fluids and solids encapsulated under extreme pressure-temperature condition. The process begins when an acoustic wave is photoelastically launched from a metal transducer. A time-of-flight delayed cylindrical probe beam scatters of off the transducer and a traveling wave. These two diffracted fields mix in an analogous way to Thomas Young's double-slit experiment, except here one slit travels at the SoS of the sample medium. The optical field emission (wave interference) provides a continuum of measureable ultrasonic frequencies. Aperture selection of a small scattering wavevector range enables collection of signal with sufficient phase coherence to determine the SoS with > 99.5 % accuracy. Here we employ PALS to study a fluid boron oxide within a heated diamond-anvil cell in order to develop and stringently test equation of state based thermochemical predictions.